LIMNOLOGY and OCEANOGRAPHY

ASLO

Limnol. Oceanogr. 68, 2023, 2492–2511

doi: 10.1002/lno.12437

Vertical niche occupation and potential metabolic interplay of microbial consortia in a deeply stratified meromictic model lake

Pedro J. Cabello-Yeves [1,2,3] **Antonio Picazo,** [1] **Juan J. Roda-Garcia,** [2] **Francisco Rodriguez-Valera** [2] **Antonio Camacho** [1*]

[1]Cavanilles Institute of Biodiversity and Evolutionary Biology, University of Valencia, Paterna, Valencia, Spain
[2]Evolutionary Genomics Group, Departamento de Producción Vegetal y Microbiología, Universidad Miguel Hernández, Alicante, Spain
[3]School of Life Sciences, University of Warwick, Coventry, UK

Abstract

The microbial ecology of meromictic lakes assessed with "omics" is still poorly studied compared to other aquatic systems. Here, a combination of metagenomics, high resolution sampling and detailed physical–chemical data gathering allowed to study the planktonic prokaryotic assemblages and metabolic capabilities in the crenogenic meromictic Lake El Tobar (Spain), a model lake for such purposes. This system presents a specific stratification comprising a freshwater layer and a halocline linked to the oxycline, driving to the euxinic hypersaline waters of the deep monimolimnion. The different strata showed a highly diverse and vertically distributed microbiome with their metabolic capacities fitting/influencing the physical–chemical environment. Overall, up to 338 novel genomes were found from metagenome assembled genomes. Picocyanobacteria and methanotrophs were abundant in the upper part of the oxycline. Anoxygenic phototrophs (*Chlorobium*, *Thiohalocapsa*, Chromatiaceae, *Rhodospirillum,* and Rhodobacteraceae spp.) dominated the 12.5–14 m anoxic waters with dim light availability. Sulfate reducers (Desulfobacterota and Firmicutes) inhabited low redox horizons from 13.5 to the bottom (18 m). The potential microbial synergistic performance increases toward the monimolimnion. Among these, a microbial assemblage mostly composed of Spirochaetota, Cloacimonadota, Omitrophota, Firmicutes, Marinisomatota, Nanoarchaeota, and Patescibacteria in hypersaline waters of 14–18 m (conductivities of 118–213 mS cm^{-1}), is potentially capable of performing mixed-acid fermentations, even including hydrogen and butanol biosynthesis of biotechnological interest. This metagenomics study shows how microbial lifestyles may be determinant in the interplay of environmental gradients, and exemplifies the potential interactions between the microbial guilds thereby.

The study of the microbial ecology of meromictic lakes started in the 19th century, when Sergei Winogradsky designed a specific device (Winogradsky column) to study the nutrient cycling, stratification, and succession of microorganisms. Meromictic lakes, though they are relatively rare, are distributed worldwide, but among them, crenogenic meromictic lakes, such as the lake here studied, are even more scarce (Gulati et al. 2017). However, among all existing aquatic habitats, meromictic lakes are key ecosystems to study bacterial/archaeal diversity in different interphases, where oxic and anoxic layers are permanently separated by a chemocline that forms redox, nutrients, dissolved gases, and often salinity gradients (Zadereev et al. 2017). The suitability for the study of these gradients and the possible functional interlinks among aquatic microbes, and how they alter the environment, make meromictic lakes ideal ecosystems for the study of microbial interactions and gradient environmental biogeochemistry, even to understand the evolution of life on Earth (Camacho et al. 2017).

Here, we present one of the most detailed studies relating the vertical zonation of the environmental features and the

*Correspondence: antonio.camacho@uv.es

Additional Supporting Information may be found in the online version of this article.

Author Contribution Statement: A.C. and F.R.-V. conceived the study. P.J.C.-Y., A.P., A.C., and F.R.-V. took the water samples. P.J.C.-Y., A.P., and J.J.R.-G. performed DNA extraction. P.J.C.-Y. and A.P. analyzed the sequence data. A.C. and F.R.-V. provided the funding. P.J.C.-Y., A.P., and A.C. wrote the manuscript. All authors read, provided comments and approved the manuscript.

microbial assemblages performed so far in any meromictic lake, focused on the crenogenic meromictic Lake El Tobar (Spain) taken as a model lake to shed light on how the interactions among microbes (according to their ecophysiological capacities determined by metagenomics) and with their environment shape the vertical distribution of microbial assemblages and the environmental conditions thereby. Lake El Tobar is an epicontinental karstified system formed by the solution and sink of a combination of Cretaceous dolomites and Triassic salt-rich "Keuper" (Barreiro-Lostres et al. 2015). The lake presents two basins, but only one (18 m of max. depth) presents a crenogenic meromixis (Vicente et al. 1993). One of the peculiarities of this system is the formation of a strong salinity (as shown by conductivity) gradient from the 0.6 mS cm^{-1} surface freshwaters to the > 200 mS cm^{-1} hypersaline bottom waters. A permanently anoxic, saline monimolimnion, starting at around 14 m and reaching the bottom at 18 m occupies the deepest lake waters. Several limnological, molecular, and physiological studies, framing the previous knowledge for our study, have been derived from this unique lake: these include, for example, the study of the factors influencing plankton layering (Miracle et al. 1993), the vertical microstratification of green and purple sulfur bacteria (Garcia-Gil et al. 1999; Camacho et al. 2002), as well as the vertical distribution and migration of *Daphnia* (King et al. 1995; Boronat and Miracle 1997).

Other meromictic lakes have been studied in detail for years using different molecular and ecological approaches. For instance, Lake Cadagno, a well-known lake displaying a strong stratification of planktonic microorganisms driving vertically contrasting rates of the metabolic processes (Camacho et al. 2001; Tonolla et al. 2017), is a representative example from which amplicon sequencing studies have subsequently been derived (Danza et al. 2018; Saini et al. 2022). Both phototrophic sulfur bacteria and sulfate-reducers (Desulfobacterota) are extremely abundant in these systems (Storelli et al. 2013) and have also been studied in this lake (Danza et al. 2017; Di Nezio et al. 2021; Philippi et al. 2021). Another 16S rRNA amplicon sequencing approach was applied to study both carbon and sulfur cycles below the chemocline in Mahoney Lake in British Columbia (Hamilton et al. 2016). The different strata of two hypersaline meromictic Romanian lakes (Ursu and Fara Fund) were also studied with this approach (Andrei et al. 2015), and a recent work described in more detail Ursu Lake, a freshwater-to-hypersaline, oxic-hypoxic-euxinic system from which a recent metataxonomic study was released (Baricz et al. 2020).

In recent years, an increasing number of metagenomic datasets from freshwater ecosystems have been added to the databases. These included the largest oxic and bathypelagic freshwater system, Lake Baikal (Cabello-Yeves et al. 2018, 2019), Rift African Valley lakes holding an anoxic hypolimnion, such as Lake Tanganyika (Tran et al. 2021) and several other European (Ghai et al. 2014; Cabello-Yeves et al. 2017; Mehrshad et al. 2018), Asian (Okazaki et al. 2019) and North-American (Linz et al. 2018; Tran et al. 2018; Buck et al. 2021) natural lakes and artificial reservoirs. Saline soda lakes have also been described in the last years using a metagenomic approach (Vavourakis et al. 2018, 2019). However, among all the above mentioned cases, meromictic lakes, and, particularly, crenogenic meromictic lakes such as Lake El Tobar, remain largely unexplored by metagenomic approaches. A handful studies have shown up in the last decade, for instance, complex microbial populations were depicted from the meromictic Ace Lake in Antarctica (Lauro et al. 2011; Yau et al. 2013), and a model studying the different strata from this lake during ice and ice-free seasons has been developed (Panwar et al. 2020). Recently, microorganisms thriving in Lake Bolshie Hruslomeny were sequenced (Kadnikov et al. 2019), metagenomes from Lake Pavin showed new microbes involved in methane cycle (Biderre-Petit et al. 2019), and new viral and microbial interactions were studied in Lake Shunet in Siberia (Wu et al. 2018).

Microbes inhabiting permanently stratified meromictic lakes, and their potential ecophysiological links, remain poorly known at the genomic level. Only some genomes from purple and green sulfur bacteria (PSB and GSB) anoxygenic photosynthesizers have been recently sequenced and analyzed. Among them, it is noticeable the purple sulfur bacterium *Chromatium okenii* sequenced from Lake Cadagno (Luedin et al. 2019), as well as the genomes of *Thiohalocapsa* sp. ML1 (Hamilton et al. 2014) and the green sulfur bacterium *Chlorobium tepidum* TLS (Eisen et al. 2002). Most recently, a study focused on freshwater Chlorobia metagenome assembled and single-cell amplified genomes (MAGs and SAGs), which were obtained all around the globe (Garcia et al. 2021). Other genomes such as those of *Lamprocystis purpurea* DSM 4197, *Chlorobium limicola* DSM 245, *Chlorobium phaeovibrioides*, or *Chlorobium ferrooxidans* have been made available from US DOE Joint Genome Institute. The latter is particularly interesting, as its capacity to perform iron-driven anoxygenic photosynthesis (Camacho et al. 2017) in the modern Archaean ocean iron-rich analog meromictic lake La Cruz, in Spain (Walter et al. 2014) has been recently demonstrated. Apart from these well-known abundant phototrophs, other microorganisms linked to the sulfur cycle, such as sulfate-reducers (Desulfobacterota and Firmicutes) have been widely found in these systems (Tonolla et al. 2000; Peduzzi et al. 2003; Kubo et al. 2014) although not described at the genomic level until a recent survey that analyzed hundreds of desulfobacterota MAGs (Langwig et al. 2021).

However, all the uncultured taxa forming microbial consortia associated to anoxygenic phototrophs and sulfate-reducers remain largely unknown in these ecosystems. From what we discovered from the study of the community structure of Lake El Tobar, such assemblages may include the presence of recently described phyla such as Nanoarchaeota and Patescibacteria (Anantharaman et al. 2016; Castelle et al.

2018), Cloacimonadota (Hamilton et al. 2016; Dyksma and Gallert 2019), Marinimicrobia (Bertagnolli et al. 2017), Spirochaetota (Graber and Breznak 2004; Dong et al. 2018), Acetothermia/Bipolaricaulota (Youssef et al. 2019), Synergistota (Riviere et al. 2009), all of which have been described from diverse anoxic environments and may have substantial roles in syntrophic microbial networks (McInerney et al. 1981; Schnürer et al. 1996; Harmsen et al. 1998) with syntrophic co-cultures (Summers et al. 2010; Dyksma and Gallert 2019), sulfate-reducers and/or methanogens (Hattori 2008; Stams and Plugge 2009; Skennerton et al. 2017), where they might display diverse fermentation (including mixed-acid) and hydrogen production metabolisms.

This study was particularly motivated by the paucity of metagenomics from continental meromictic lakes, relating the microbial communities, their functions and their physical and chemical environment. To this end, we have generated a fine profile of a crenogenic meromictic lake that is ca. four times more saline than the sea in its monimolimnion. Remarkably, this lake presents a huge gradient of salinity from the deepest part of its epilimnion, where the deep-chlorophyll-maximum (DCM) is located, to the bottom of the monimolimnion. Under this gradient, which is linked to another in physical and chemical features, the microbial inhabitants of each stratum were identified, including those unique from the freshwater layer and those thriving in the transition to more saline waters within the same lake. To complete our study, we have studied the major ecological factors changing in the vertical gradient, then related them with the most relevant taxa and their metabolic capacities unveiled through Metagenome Assembled Genomes (MAGs), analyzed their potential biogeochemical key roles in the ecosystem, and provided a model for a very specific niche adaptation to the depth-growing harsh saline and euxinic conditions of this peculiar lake used as a model for the knowledge of spatial patterns and ecological interactions among microorganisms, and of these with their environment.

Methods

Sampling and physical and chemical profiles measurement

Lake El Tobar was sampled on July 9, 2019, when thermal stratification of upper layers is added to the permanent crenogenic meromixis. Detailed vertical profiles of physical and chemical variables were obtained with a CTD probe (SeaBird 19) set up with different sensors. CTD was equipped with specific sensors for pressure, conductivity, and temperature. Further, the probe was fitted with sensors for oxygen (SB-43), chlorophyll a (Chl *a*; fluorimetric, Wetstar), phycoerythrin (fluorimetric, Seapoint), phycocyanin (fluorimetric, Cyclops-7 Turner), pH and ORP (SBE27), CDOM (fluorimetric, Wetlabs), and turbidity (Seapoint). Values of Eh′ (redox potential with respect to the standard hydrogen electrode and corrected to pH 7) were calculated from ORP according to the manufacturer's instructions following previous approaches (Wetzel 2001). A single sampling point located on the deepest point of the meromictic basin of the lake was chosen as representative of the different water column strata based on the "in situ" acquired physical and chemical profiles, and were set at 2, 12, 12.5, 13, 13.5, 14, 15.5–16.5 (integrated and obtained with a Rutter bottle) and 18 m of depth. The samples (single replicates) were obtained from a boat, moored over the deepest point of the monimolimnion basin, by using inverted double cone fine-layer sampling device with a vertical resolution of ca. 5 cm (Miracle et al. 1992) to obtain a stable laminar flux, connected to a battery-driven peristaltic pump. This sampling device was particularly designed to minimize vertical disturbance and allowed to obtain samples at well-defined layers (Camacho et al. 2003). Previous profiles from the lake have been obtained in Vicente et al. 1993, Garcia-Gil et al., 1999; Camacho et al., 2002.

Chemical and photosynthetic pigment analyses

Analytical water measurements of alkalinity, nitrate, ammonia, sulfate, and phosphate were conducted following standard methods (APHA 2005). Alkalinity was analyzed from unfiltered samples by titration with HCl using a pH shift indicator (phenolphtalein) of the equivalence end point pH (method 2320; APHA 2005 [APHA AWWA 2005]). Analyses of nitrogen and phosphorus fractions were conducted following spectrophotometric methods using a Beckman DU-7 UV–Visible spectrophotometer. Thus, soluble orthophosphate (PO_4) was analyzed by the ascorbic acid method (method 4500-E; APHA 2005 [APHA AWWA 2005]). Nitrate (NO_3) was measured by the second derivative UV/Visible spectroscopy method (method 4500-C; APHA 2005 [APHA AWWA 2005]). Ammonia (NH_4) was determined using a modification of the phenate APHA method using salicylate instead of phenol (Golterman 2004). Photosynthetic pigments (Chl *a*, Chl *b*, Bchl *a*, and Bchl *e*) concentration was quantified by liquid chromatography (HPLC) following Picazo et al. (2013) using a Waters HPLC system equipped with a Waters 996 photodiode Array Detector. Pigment recognition and calibration were made by comparing retention times and spectra with those of pure standard (DHI, Denmark).

Bacterioplankton analyses by flow cytometry

Heterotrophic bacterioplankton (HPP), picocyanobacteria (APP), Green (GSB) and purple sulfur bacteria (PSB) counts were performed using a Beckman Coulter flow cytometer (Cytomics FC 500 MPL) with five fluorescent channels equipped with an argon laser emitting at 488 nm. The Beckman Coulter Cytomics FC 500 worked with two lasers, an air-cooled Argon ion laser, 488 nm (20 mW output), and a second air-cooled Helium–Neon ion laser, 633 nm (20 mW output). Argon laser beam spot size was 10 μm high by 80 μm wide (elliptical) and Helium–Neon laser beam spot size:

9.5 μm high by 85 μm wide (elliptical). Regarding the detectors, the forward scatter and side scatter detectors were photodiodes and we use the five photomultipliers (FL1-FL5) with spectral sensitivity from 185 to 900 nm for collect the fluorescence signals with a Band Pass (BP): 525 nm (FL1), 575 nm (FL2), 620 nm (FL3), 675 nm (FL4), and 755 nm (FL%). The dichroic long pass (DL) was 488, 550, 600, and 710 nm. The dichroic short pass (DS): 615 and 645 nm. The long pass (LP) is 500 nm and short pass (SP) 620 nm. Samples were fixed in PBS buffered paraformaldehyde : glutaraldehyde solution to a final concentration in the sample of 1 : 0.05% (Marie et al. 1997) and incubated for 30 min at dark. For heterotrophic bacteria counts, bacterial cells were stained with SYBR Green-I (C32H37N4S). Data were visualized in plots of side scatter light (SSC channel) vs. fluorescence (FL1 channel) channels, which corresponds to the cell complexity and fluorescence emission of SYBR Green-I. For photosynthetic microorganisms, picocyanobacteria, purple and green sulfur bacteria, pigment autofluorescence were used to discriminate populations, using FL2 (phycocyanin), FL4 (chlorophyll), and SSC (size) for picocyanobacteria, and FL5 (Bacteriochlorophyll) and SSC (size) for green and purple sulfur bacteria. Data were acquired in log mode and for each depth at least 2 analyses were performed according to the different abundances of the populations studied, being the first analysis for heterotrophic bacteria and the second one for photosynthetic organisms. Fluorescent beads of 1 μm size were used to calibrate cell complexity. Total bacteria were calculated as the sum of heterotrophic bacteria, picocyanobacteria, green and purple sulfur bacteria.

DNA extraction, sequencing, assembly, and read annotation

DNA from eight single replicate samples (2, 12, 12.5, 13, 13.5, 14, 15.5–16.5, and 18 m of depth) was extracted with phenol–chloroform methodology (Martín-Cuadrado et al. 2007). In short, filters were treated with CTAB lysis buffer and then treated with 1 mg mL^{-1} lysozyme and 0.2 mg mL^{-1} proteinase K (final concentrations). Then nucleic acids were extracted with phenol/chloroform/isoamyl alcohol and chloroform/isoamyl alcohol. The eight samples were sequenced in an entire lane of Illumina HiSeq X Ten PE 2X150 bp (BGI company), which provided ca. 120 million clean reads and 15 Gb of output for each sample. Samples were individually assembled with IDBA-UD (Peng et al. 2012) with the parameters—pre_correction, -mink 50, -maxk 140, and -step 10. Sub-assemblies of 20 million reads were done in each sample to retrieve some of the most abundant microbes that assembled poorly by using all sequenced reads, hence we reduced the total number of reads to obtain more complete bins of these representatives. Annotation of contigs was assessed using Prodigal (Hyatt et al. 2010) for ORF prediction and then top hits (> 30% of identity and > 50% of query coverage) of each individual protein were determined using Diamond blastp (Buchfink et al. 2015) against the NCBI Nr (January 2022) database. HMMs were generated for COGs (Tatusov et al. 2001) and TIGRFAMs (Haft et al. 2001) databases and these were used to determine further protein annotations above the threshold inclusion values from HMMscan. All information combined was used to provide the most updated NCBI taxonomy and product information (Nr, COG, TIGRFAM) for each particular protein. Features like tRNAs and rRNAs were detected with tRNAscan (Lowe and Eddy 1997) and ssu-align (Nawrocki and Eddy 2010), respectively.

Binning, classification, and features of MAGs

Binning procedure was performed as follows: a first manual inspection was done assigning a hit (based on BLAST against Nr) to each CDS, which allowed us to classify each of these taxonomically into different phyla. Contigs with > 50% of their CDSs belonging to a particular phylum were pooled together for further analysis. Then, an initial binning step was applied for each set of contigs assigned to each phyla with METABAT2 (Kang et al. 2019) using coverage mapping individual reads vs. contigs with Bowtie2 (Langmead and Salzberg 2012) in the different samples. Further manual contig inspection was applied using GC and tetranucleotide frequencies (wordfreq package from EMBOSS) and Principal components analysis (FACTOMINER package in R) to refine the bins (Rice et al. 2000; Lê et al. 2008). Finally, we only used MAGs with < 5% contamination and > 50% of completeness estimated by CheckM package (Parks et al. 2015). Even if MAGs belonging to the same species were generated from different depths, we did not dereplicated them and instead we kept them separately to assess differences in gene presence/absence, flexible genome and other polymorphisms between different depths in future studies. MAGs were classified according to the latest version of GTDB (Parks et al. 2018) and whenever we could we used class, order, family, genus, or species names for all of them.

16S rRNA read classification, hierarchical cluster read analysis, read functionality, and isoelectric points of the predicted metaproteomes

The 16S rRNA gene reads from the different metagenomes were obtained using a sub-set of 20 million reads. We first obtained candidates with USEARCH (Edgar 2010) with RefSeq 16S rRNA database and then these putative were confirmed using ssu-align (Nawrocki and Eddy 2010). Then, a BLASTN was performed against the last version of SILVA database (Quast et al. 2012) (SILVA138.1) to provide a taxonomic classification. Only top hits at > 75% of sequence identity and coverage were used in this analysis. Hierarchical cluster analysis (dendrograms) of different metagenomic samples with k-mer = 21 bp was assessed with SIMKA (Benoit 2015) and Bray-Curtis indices based on presence/absence data were obtained.

Subsets of 20 million reads of each metagenomes were analyzed with BLASTX against SEED (comparative genomics and

annotation environment) subsystems (Overbeek et al. 2013) database with Diamond (Buchfink et al. 2015), with options more-sensitive, max-target-seqs 1, e-value 0.00001 > 50 bp of alignment length and > 50% identity. The top hits were analyzed in search of specific genes and pathways based on the SEED database. Hits were normalized by the total number of hit counts for each sample and a row *Z*-score was calculated to assess statistical differences between samples for each metabolic pathway. Finally, to determine the whole-proteome isoelectric points (pIs) on each sample we obtained all those proteins from contigs > 5 Kb and calculated their pIs with Pepstats from the emboss package (Rice et al. 2000).

Metabolic pathways estimation for MAGs

To predict the key roles of our different retrieved bacterial and archaeal genomes we annotated them with the same abovementioned tools for contig annotation plus individual MAG annotation with RAST (Overbeek et al. 2013), Kegg-KO (Kanehisa and Goto 2000), CDD-SPARCLE (Marchler-Bauer et al. 2016) databases and BLAST Koala (Kanehisa et al. 2016) to assign KEGG-KO genes. We constructed gene/protein presence/absence tables for metagenomes and individual microbes based on SEED and we relied on database annotations for each MAG as described above.

Relative abundance of MAGs

To estimate the relative abundance of the recovered genomes we performed read recruitment and mapping, which was assessed considering BLASTN hits of the MAG into the metagenomic reads at > 95% identity and 50 bp of alignment length, as belonging to the same species. A microbe was considered present in a metagenome if it was detected at > 2 RPKG (Reads per Kb of Genome per Gb of Metagenome). All the RPKG values for the most abundant MAGs retrieved from this work on the different depths of Lake El Tobar metagenomes are shown in Supplementary Table S3. For this particular analysis, we used a single dereplicated representative/species (> 95% of ANI) to determine abundances (see Fig. 5; Supplementary Table S3), thus avoiding overestimation for both the coverage and the relative abundance. To assess the intraspecific and interspecific diversity we showed recruitment plots at > 80% of identity/50 bp alignment lengths.

Redundancy analysis (RDA) of environmental variables, MAGs, and metabolic processes

A distance-based redundancy analysis (dbRDA) analysis was performed to describe the ordination of the main MAGs and metabolic processes in an environmentally constrained space (Legendre and Anderson 1999). This was conducted with the vegan R package. An environmental variables matrix with 16 environmental plus microbial abundance variables (Supplementary Table S1) for the eight studied depths of Lake El Tobar was used (temperature, conductivity, pH, Eh', dissolved oxygen, PAR, CDOM, turbidity, alkalinity, nitrate, ammonia, sulfate, phosphate, Chl *a*, bacteriochlorophyll-a, bacteriochlorophyll-e, phycocyanin, and total bacteria). The environmental matrix was square root transformed and normalized before building a Euclidean resemblance matrix. On the other hand, recovered genomes (MAGs) matrices with the main 64 MAGs (Supplementary Table S3), and metabolic processes matrices with 52 selected metabolic processes were used (Supplementary Table S4), both were standardized and square root transformed before performing a Bray–Curtis dissimilarity resemblance matrix. The first dbRDA was performed with the recovered genomes (MAGs) matrix using environmental matrix as predictor variable, and the second dbRDA with de metabolic processes matrix using environmental matrix as predictor variable.

Availability of metagenomes and MAGs

All objects derived from this work are publicly available under the NCBI Bioproject number PRJNA639779. Metagenomes were deposited to NCBI-SRA numbers SRR12088346- SRR12088352. Biosample accession numbers for all MAGs were assigned accordingly from SAMN21020239-SAMN21020591 and Genbank accession numbers to JAIOWS000000000-JAIPKG000000000.

Results

Environmental variables driving the crenogenic meromixis and the vertical distribution of microbes

A total of eight depths were sampled providing an overview of the differential and most significant ecological environments in Lake El Tobar according to the different variations in conductivity, temperature, chlorophyll/bacteriochlorophyll, dissolved oxygen, and nutrients (chemistry) measured in situ (Fig. 1; Supplementary Table S1). A representative sample of the freshwater epilimnion was taken at 2 m. The sample of 12 m corresponded to the freshwater oxycline (1.3 mS cm^{-1}). The deepest oxic/anoxic interface corresponded to the sample of 12.5 m, with 10.9 mS cm^{-1} where the second oxygen extinction was observed (Fig. 1). The Deep Chlorophyll Maximum (DCM) was located under the deep oxygen maximum between 12.5 and 13 m (27.4 mS cm^{-1}); then, the 13 m sample corresponded to the bottom of the deep chlorophyll maximum. Another sample corresponding to the saline hypolimnion was taken at 13.5 m with higher conductivity (67 mS cm^{-1}). The start of the monimolimnion (14 m) overlapped the Eh' drop and conductivity rise to values of ca. 118 mS cm^{-1}. We also obtained an integrated sample of 15.5–16.5 m, which already corresponded to the upper aphotic saline monimolimnion (170 mS cm^{-1}). Finally, we obtained the deepest sample at 18 m, corresponding to the deep aphotic saline monimolimnion (> 200 mS cm^{-1}) close to the sediment, though avoiding mixing with sediments. The highest bacterial biomass, both autotrophic and heterotrophic, was found between 12 and 15 m in the confluence of the light depletion and salinity increase gradient zone (Supplementary Table S1).

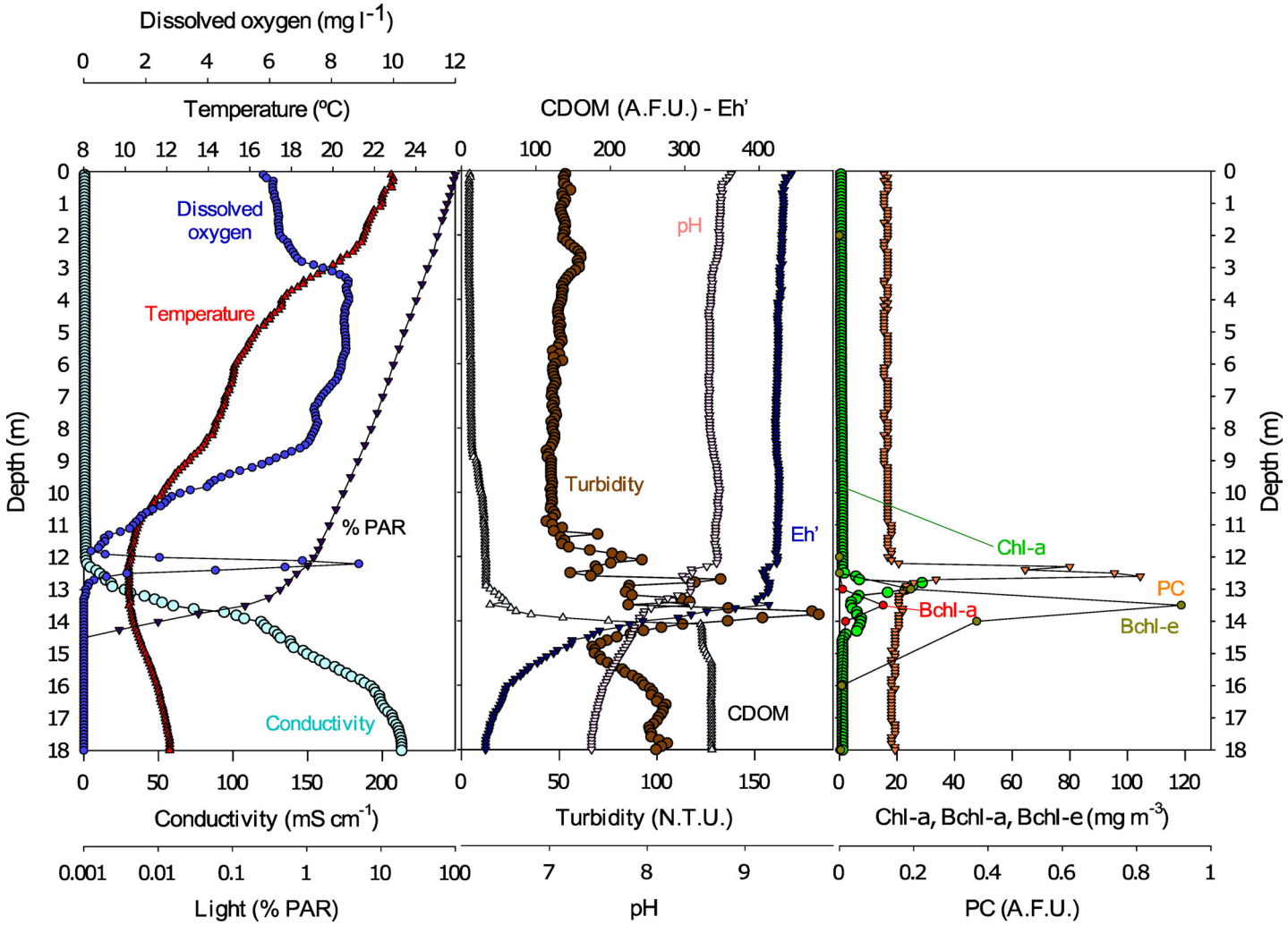

Fig. 1. Vertical profiles of physical and chemical variables and photosynthetic pigments concentrations in Lake El Tobar at the sampling date (July 2019). Each variable is color and shape coded. Eh′ = redox potential, PC = phycocyanin, Chl *a* = chlorophyll *a* and Bchl (*a* or *e*, respectively).

The vertical distribution of the concentrations of the main photosynthetic pigments that can be used as biomass proxies for phototrophic microorganisms, and the abundance of both autotrophic (APP, picocyanobacteria) and heterotrophic (HPP) picoplankton, respectively, as well as that of purple and green sulfur bacteria (Fig. 1; Supplementary Table S1), indicated a fine stratification of these communities in the water column along these gradients. The increase of the light extinction coefficient (%PAR slope) from 12 m (1.2% PAR) up to light extinction at 14.5 m marked the most important zone of distribution of the main photosynthetic prokaryotic microorganisms (picocyanobacteria, purple and green sulfur bacteria). This most productive layer coincided with the zone where the highest abundance of heterotrophic picoplankton was observed (around 14 m). Dissolved phosphorous, ammonia, and sulfate gradually increased with depth, showing their maximum at the monimolimnion at 18 m (Supplementary Table S1).

Metagenomics profile: Main MAGs, taxonomic, predicted proteomes, and metabolic features

The strong contrast in the main physical, chemical features, and different biotic zones in the water column profile of the lake led us to generate a metagenomics profile. We applied a raw read, 16S rRNA and predicted proteome analysis (Fig. 2). Remarkable differences in the prokaryotic community structure between layers were observed (Fig. 2a; Supplementary Data S1) using unassembled metagenomics 16S rRNA gene reads. Briefly, the epilimnion (2–12 m) was clearly dominated by Actinobacteria from the acI lineage, cluster 5 picocyanobacteria (Synechococcales) and Gammaproteobacteria (Burkholderiales order). Samples from 12.5 to 13 m showed a high abundance of Alphaproteobacteria from Rhodospirillales order (see Data S1). The 13.5 m sample presented the highest abundance of anoxygenic phototrophs and in the 14 m sample there was a bloom of Cloacimonadota. Finally, the monimolimnion was

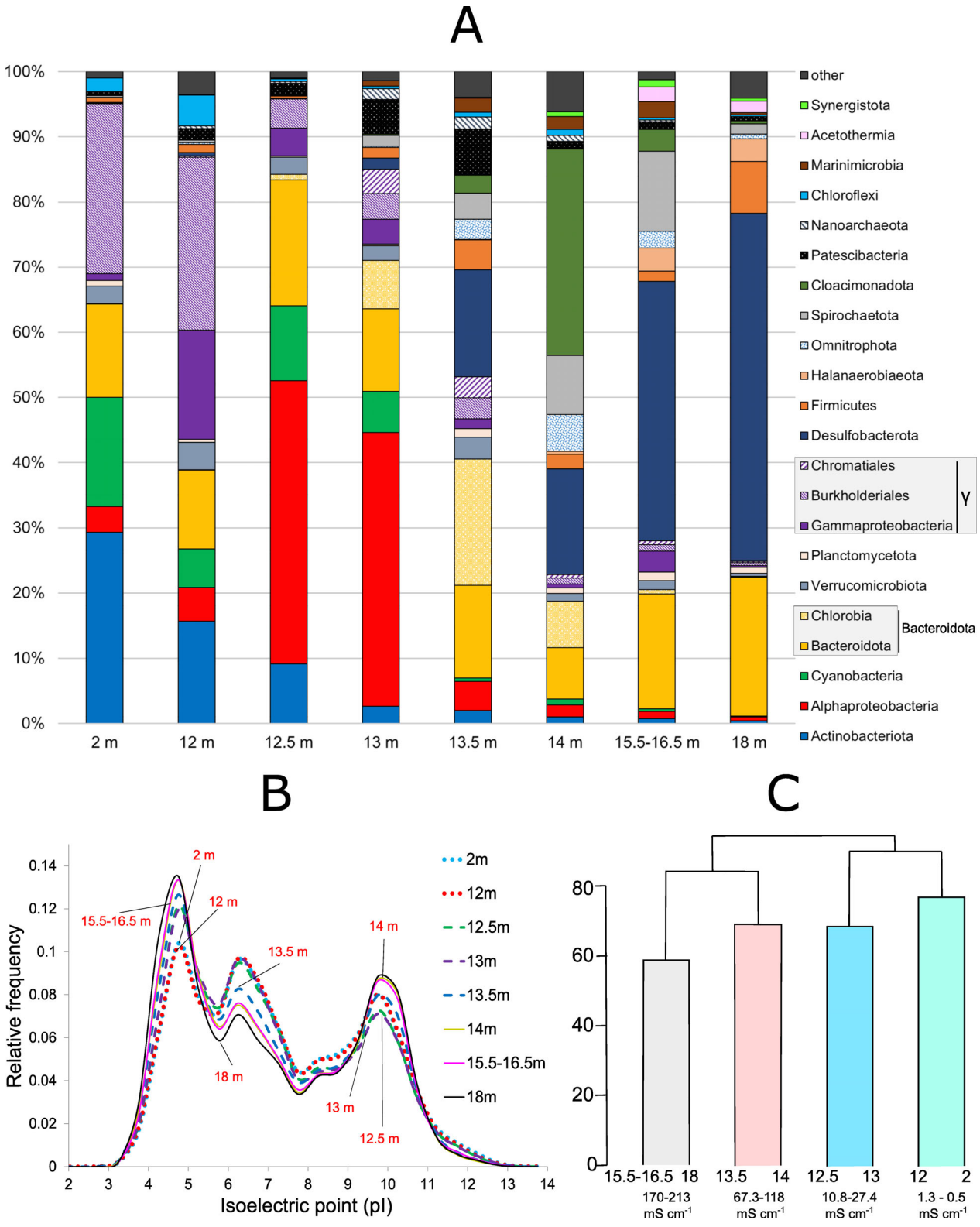

Fig. 2. Metagenomic read analysis of the different layers of the meromictic Lake El Tobar. (**a**) Taxonomic 16S rRNA gene read classification. Phyla are color coded. Orders Burkholderiales and Chromatiales were counted separately from other Gammaproteobacteria to assess specific differences between them. Chlorobia was also separated from Bacteroidota. (**b**) Whole-proteome isoelectric points (pIs) patterns for each depth. We used between 80 and 240 K predicted proteins for each sample. (**c**) Hierarchical read cluster analysis based on a Bray-Curtis matrix. Y axis represents read dissimilarity and X axis shows the sample (depth) clustering and the conductivity range within the clustered lake layers.

mostly dominated by sulfate reducers from Desulfobacterota phylum (see Data S1). A functionality profile was produced to discriminate the key and most prevalent metabolic pathways of each stratum (see Supporting Information Fig. S1 in Data S1), that was ultimately correlated with the taxonomic pattern obtained from 16S rRNA gene reads (Fig. 2a) and the MAGs genomic context.

To assess potential functional differences between strata influenced by the salinity gradient we obtained the predicted whole-proteome isoelectric point (pI) patterns from each whole-assembled sample (Fig. 2b). Here, a gradual increase of acidic pIs (3–5) and a progressive decrease of neutral/basic pIs (7–9.5) was observed as salinity/conductivity increased in the water column. Freshwater samples with lowest conductivity (epilimnion at 2 m and oxycline at 12 m, from 0.5–1.3 mS cm^{-1}) had the less acidic and highest neutral and basic pIs (from 7 to 9.5). Layers of intermediate salinity such as the deep chlorophyll maximum and the hypolimnion (10.9–67.3 mS cm^{-1} from 12.5 to 13.5 m) had intermediate pI values at all acid, neutral, and basic peaks. Finally, the most saline samples, that corresponded to the monimolimnion (118–213 mS cm^{-1} from 14 to 18 m) and showed an acid shift on their hypothetical proteomes and a notable decrease in neutral to slightly basic proteins, confirming a pattern linked to the salinity increases with depth reaching up to four to five times the salinity of marine waters in the Lake El Tobar deepest waters. The hierarchical cluster analysis showing Bray–Curtis presence/absence dissimilarity with reads (Fig. 2c) confirmed the trend showed by the taxonomic 16S rRNA assignment and predicted whole-proteome analysis. Freshwater samples clustered together, which indicates a similar taxonomic build up. Intermediate salinity sub-oxic (nearly anoxic) samples of 12.5 and 13 m also showed highest similarities among themselves. Finally, anoxic 13.5–14 m and anoxic monimolimnetic hypersaline samples from 15.5 to 18 m clustered together.

Pertinent to genome reconstruction, a total of 353 MAGs that followed the rule of > 50% of completeness and < 5% of contamination were obtained. Their main features are summarized in individual detail in Supplementary Table S2 and Data S1. Most MAGs (338, ca. 95%) were identified as novel genomes based on GTDB criteria with a total of 189 (ca. 60%) assigned to novel genus.

Linking microbial abundance, environmental parameters, and metabolic processes between strata

The differences among the different strata assessed by taxonomy, read clustering, metaproteomes and read functionality were also studied including the simultaneous multivariate analysis of environmental parameters (Supplementary Table S1) and relative abundances of the retrieved genomes (Fig. 3). A dbRDA was performed for the eight samples between the physical–chemical and microbial abundance variables and the values of relative abundance obtained for each MAG assessed by RPKGs (Reads per Kb of Genome per Gb of metagenome) (Fig. 3a) and the values of relative abundance for each metabolism (Fig. 3b) as described for Supplementary Fig. S1. Most of the observed differences shown by the abundance of MAGs (Fig. 3a) and metabolisms (Fig. 3b) could be explained by the first axis (dbRDA1), showing ca. 46.6% and 82.1% of the total variation, respectively. The second axis (dbRDA2) explained 28.8% of the abundance of MAGs and 10.1% of the total variation of metabolisms, respectively. The first axis of both dbRDAs (dbRDA1) was clearly linked to depth and the associated factors (e.g., highest salinity in deep waters). The second axis in both dbRDAs (dbRDA2) discriminated the strongest gradients area between 12.5 and 14 m linked to a greater abundance and bacterial activity, from both surface epilimnetic (2–12 m) and monimolimnetic (15.5–18 m) strata in area.

A first quadrant (freshwater epilimnion-2 m and oxycline-12 m), is featured by abundant and widespread (cosmopolitan) freshwater taxa such as *Limnohabitans, Polynucleobacter, Fonsibacter*, picocyanobacteria, and different Actinobacteria within layers. Physical and chemical associated variables were temperature, light (%PAR), dissolved oxygen and nitrate, displaying the highest values in these upper layers. The most remarkable associated metabolisms (Fig. 3b) were those typically expected for oxic photic freshwater, such as ammonia assimilation, oxygenic phototrophic metabolisms, and methane oxidation (see Data S1). Between 12.5 and 14 m, in the second and third quadrants of the dbRDA, samples show an equidistant transition between the epilimnion (2–12 m) and the monimolimnion (15.5–16.6–18 m). Most MAGs including anoxygenic phototrophs such as Rhodobacteraceae, *Rhodospirillum*, *Chlorobium*, and Chromatiales were found between 13 and 14 m, which were statistically correlated to the oxygen extinction and hypolimnetic layers coinciding with the higher abundances of photosynthetic pigments, Chl *a*, PC and bchl *a–e* (14 m). In addition, the sample of 12.5 m represents the transition to anoxia where complete oxygen extinction occurs, overlying a maximum of picocyanobacteria. At 13 m there is also a deep Chl *b* maximum that is double the amount of Chl *a* and it is related to the chlorophyte *Chlamydomonas* spp. for which ca. 60 contigs were detected recruiting average values of 44 RPKGs. The 12.5 and 13 m samples (both contributing to the deep chlorophyll maximum) are also associated with some of the novel Paceibacteria, Nanopelagicales or Woesearchaeales groups, which show a trend to the prevalence of mixed-acid fermentation pathways. Sulfate-reducers featured the monimolimnetic samples (15.5–16.6 m and 18 m), with sulfate as the most remarkable associated environmental variable. These samples are located at fourth quadrant of the dbRDA, strongly associated with high concentrations of SO_4^{2-}, organic matter, alkalinity, PO_4^{3-} (orthophosphate) and conductivity. Hydrogen metabolism and fermentations were the characteristic monimolimnetic types of metabolism linked to this complex network of microbes.

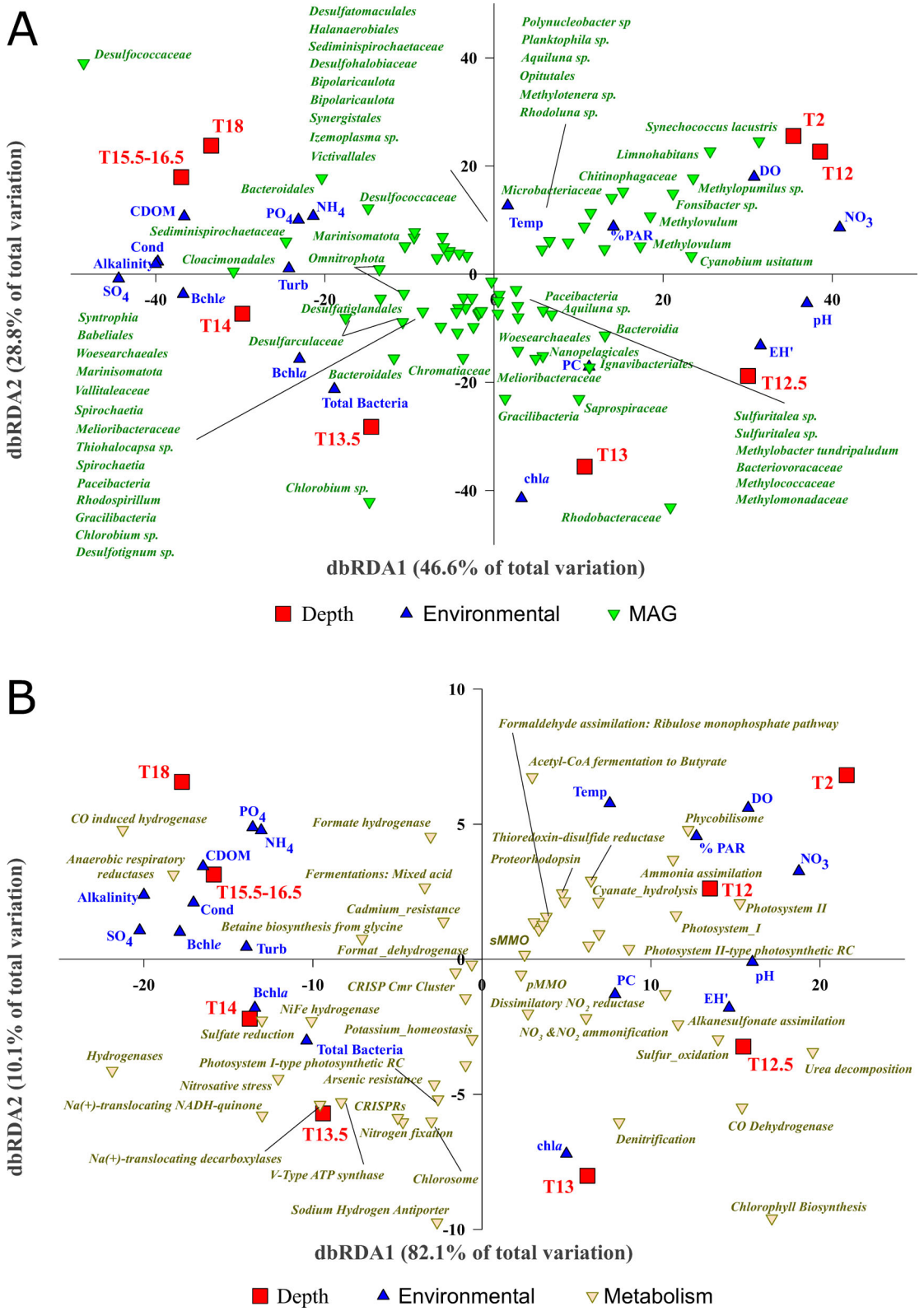

Fig. 3. dbRDA between the values of environmental and microbial abundance variables of the eight samples taken from Lake El Tobar depths, and (**a**) the MAGs generated from different depths and (**b**) the associated metabolisms. Samples, environmental and microbial abundance variables, MAGs and metabolisms are color and shape coded. Temp = Temperature; Cond = Conductivity; Turb = turbidity; DO = Dissolved oxygen; Eh' = redox potential; PC = phycocyanin, Chl *a* = chlorophyll *a*; bchla = Bacteriochlorophyll *a*.

Consortia stratification, metabolic performance, and niche adaptation

To deepen into the vertical zoning of microbes, we studied at a finer level several specific double-layers for some of the most abundant and key microbes (based on the highest RPKG values of the MAGs) of the lake (Fig. 4; Supplementary Table S3) and developed a conceptual model where we stablished the key metabolic and microbial roles for each stratum (Figs. 4, 5, 6). We also studied the population genomics of the most abundant microbes, which were found to be as nearly clonal (low species diversity) or polyclonal (high species diversity) inhabitants (Supporting Information Fig. S2).

Apart from the upper well-oxygenated photic layers, where more homogeneous environmental conditions and microbial communities were found and no biological vertical stratification was expected, the latter appeared in the depths displaying strong physical and chemical gradients. First, a double stratification of methanotrophs was observed, where *Methylovulum* spp. dominated the upper oxycline (with more than > 40 RPKG in 12 m) and the upper part of the deep chlorophyll maximum (12.5 m) layers, that is, those presenting lower salinity. On the other hand, *Methylobacter tundripaludum* and Methylococcaceae/Methylomonadaceae MAGs were found at the lower part of the deep chlorophyll maximum and the oxygen extinction at 13 m, here experiencing higher salinity (conductivity of 37.4 mS cm^{-1}). A second stratification pattern was displayed by the anoxygenic phototrophs, which were widely distributed from the upper part of the deep chlorophyll maximum at 12.5 m up to the start of the monimolimnion at 14 m, although they preferred some strata at variable salinities. For instance, a single Rhodobacteraceae species (reference MAG Tobar12.5 m-G12) was the most abundant microbe at the deep chlorophyll maximum both at 12.5 and 13 m (> 200 RPKG) and also occurred at 13.5 m. A *Rhodospirillum* sp. was less abundant (< 10 RPKG) but was found above the 16.5 m and was able to fix N. However, both species were able to produce H_2 and showed their genetic capacity for sulfur oxidation and denitrification. The stratification of the two Green sulfur bacteria (reference MAGs *Chlorobium* spp. Tobar12.5 m-G31 and Tobar13m-G12) and Purple sulfur bacteria (a *Thiohalocapsa* sp. Tobar13m-G38 and a Chromatiaceae Tobar14m-G20 as reference MAGs) differed between layers. All four species co-occurred at the anoxic hypolimnion (13 and 13.5 m), and their maximum growth and abundance was observed at 13.5 m (67.3 mS cm^{-1}), which suggests that these are well adapted to high salt concentrations. In fact, the most abundant *Chlorobium* and Chromatiaceae species (both able to perform denitrification, N fixation and S oxidation) made it to the hypersaline monimolimnion at 15.5–16.5 m although at low abundances (< 5 RPKG), and were scarce at the bottom of the lake (18 m).

Another specific stratification pattern was observed among Desulfobacterota, with very specific hypolimnetic-monimolimnetic co-occurrences or, contrarily, individual presence, all of them strictly linked to the salinity gradient. For example, Bacteriovoracaceae and Syntrophia MAGs were only present at the hypolimnion (13 and 13.5 m strata, respectively). The most abundant sulfate reducer retrieved as genome was a Desulfococcaceae (Tobar14m-G18) that recruited > 400 RPKG at the monimolimnion from 14 to 18 m. Its success probably was due to the presence of gas vesicles that would allow this microbe to move throughout the whole monimolimnion, CRISPR-Cas system for phage defense, and denitrification capacity coupled with S reduction (DSR gene cluster) that altogether conformed a very versatile genomic build-up. Desulfohalobiaceae and Desulfococcaceae spp. co-ocurred mostly at the highest salinities of 15.5–18 m (170–213 mS cm^{-1}). On the other hand, *Desulfocapsa*, *Desulfotignum* spp. were clearly concentrated at lower salinities at the 13.5–14 m layer, while Desulfarculaceae spp. covered a wider spectrum from 13.5 to 16.5 m and among their capabilities was that for nitrogen-fixation. The very specific gradient observed for Desulfobacterota exemplifies their ability perform S reduction at different salinity levels.

Remarkable variable stratifications were also observed in a sort of species from several phyla such as Spirochaetota, Omnitrophota, Cloacimonadota, Marinisomatota, Patescibacteria, Nanoarchaeota, Firmicutes, Synergistota, and Dependentiae. Our data show that these microbes coexisted with sulfate reducers (Firmicutes and Desulfobacteria), sulfur reducers, anoxygenic phototrophs (Rhodospirillales, green and purple sulfur bacteria), N fixers and denitrifiers (Bacteroidota). In this putative microbial network, these organisms are crucial to recycle organic matter and produce secondary by-products such as hydrogen, that is needed for most anaerobes thriving in this ecosystem. In particular, they were capable to produce H_2 with various hydrogenases (mostly *hox* bidirectional NiFe/FeFe) and mixed-acid fermentations, and their fermentation products were very variable depending on each microbe, including butanol as an end biosynthetic product for a few of them. For example, *Sulfuritalea* spp. only occurred in the photic layer but at different oxygen concentrations from 12.5 to 13.5 m, and their metabolic repertoire included sulfur oxidation, denitrification and dissimilatory S reduction, apart from H_2 production and fermentative pathways. Bacteroidota that spatially co-occurred with PSB and GSB included Ignavibacteriales, Bacteroidales, Melioribacteraceae, and Saprospiraceae representatives that were present in different layers, but all of them hold the denitrification pathway. It must be noted that one Cloacimonadales (reference MAG Tobar14m-G30) was extremely abundant in the upper monimolimnion at 14 m (> 400 RPKG), though it appeared throughout the bottom, being a specialist capable of performing fermentation of lactate, acetate, ethanol, formate, H_2, and CO_2. Spirochaetota are also anaerobic fermenters from which two major families were retrieved (Sediminispirochaetaceae and Spirochaetia), which occurred in all anoxic waters from 13 to 18 m with variable abundances. A specific Firmicutes (Desulfatomaculales Tobar18m-G10) was found mostly at 18 m and accompanied Desulfobacterota as the main sulfate reducers, but also

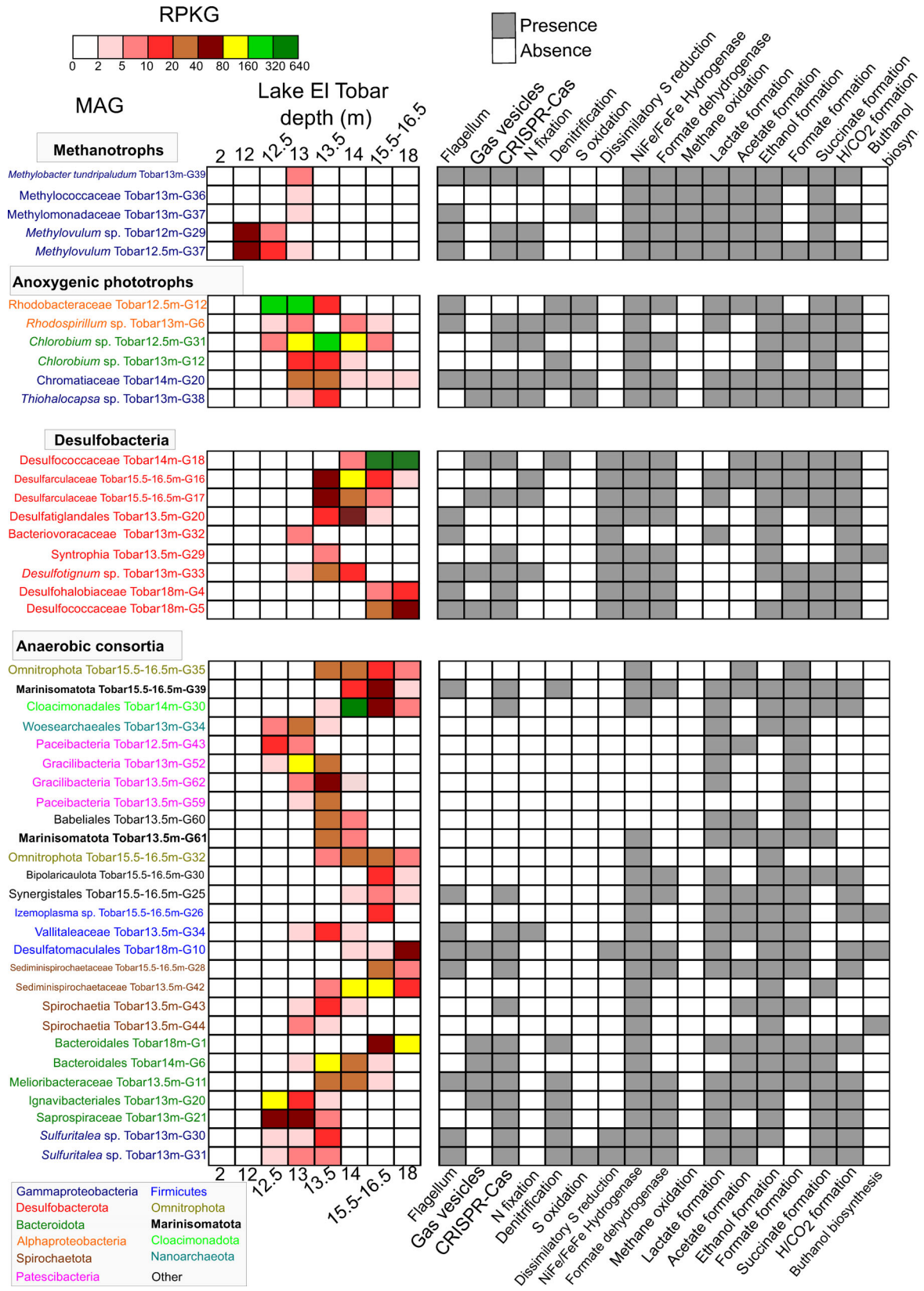

Fig. 4. Heatmap of the most abundant microbes of the lake and their associated metabolisms. Relative microbial abundances were expressed as Reads per Kb of genome per Gb of metagenome (RPKGs).

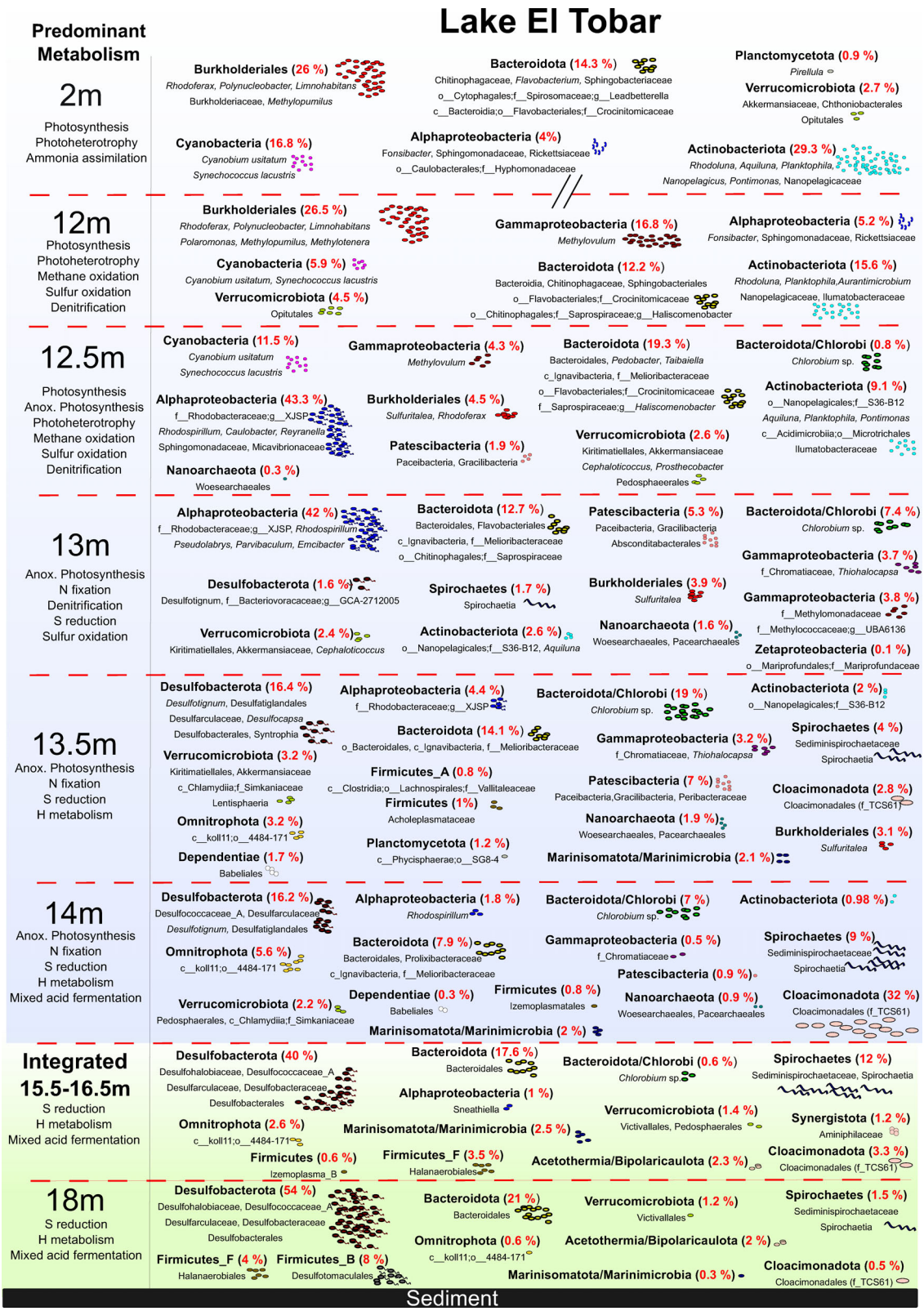

Fig. 5. Microbial spatial distribution and abundance throughout the different layers of Lake El Tobar. For each sample the most prevalent metabolisms found in MAGs are shown. Each microbial group presents in red the % of 16S rRNA reads associated for each sample and the most recent classification of the MAGs retrieved for each group assessed by GTDB. Whenever possible, we used the highest level of hierarchy and classification provided by GTDB (o_ for order, f_ for family and g_ for genus accordingly).

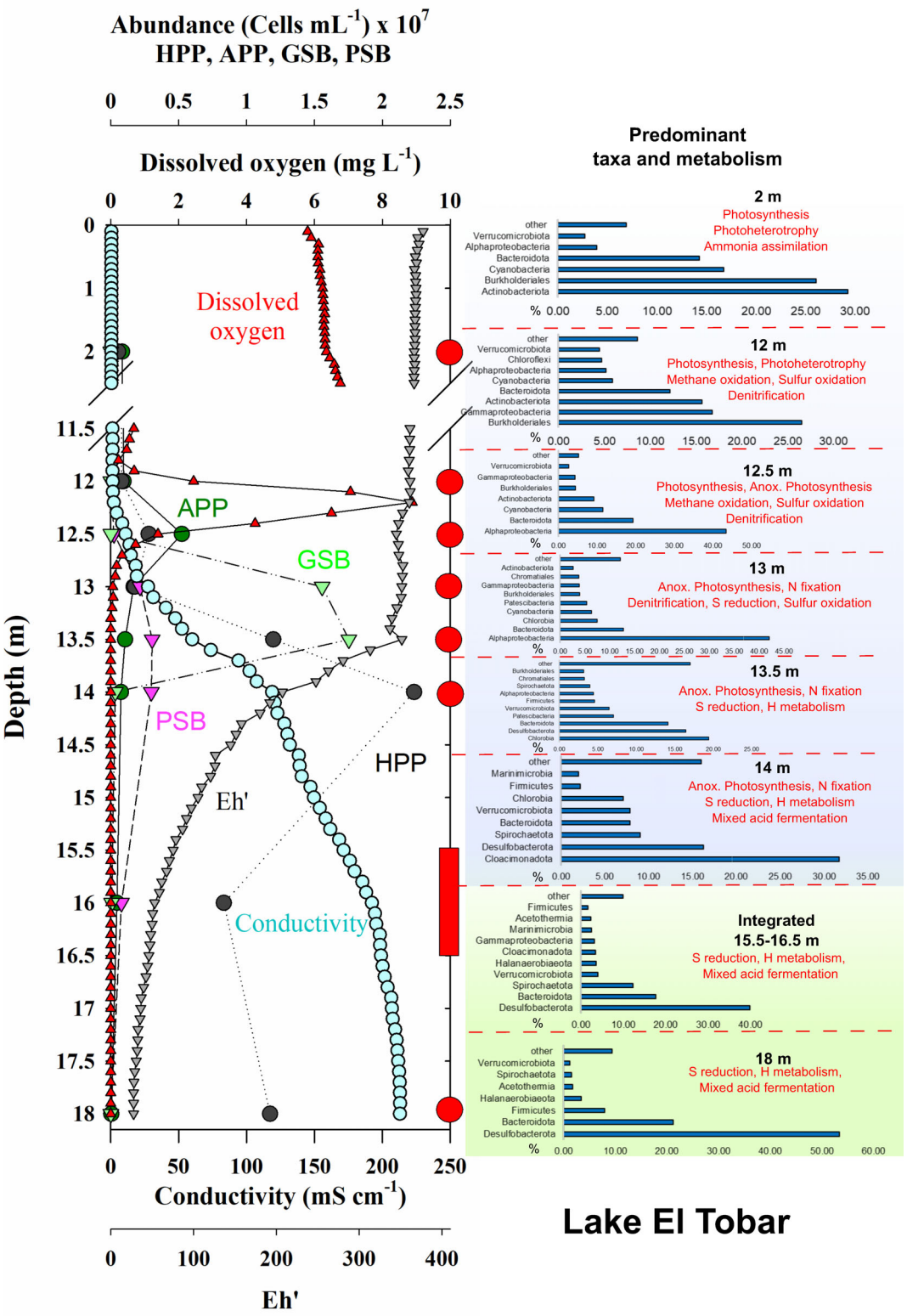

Fig. 6. Physical and chemical, taxonomic, and metabolic profiles summarizing the model chart of Lake El Tobar. Barplots for each sample correspond to the % of 16S rRNA read relative abundances. Dissolved oxygen, conductivity and Eh' are color and shape coded. A break between 2 and 12 m epilimnetic samples is shown. APP = autotrophic picoplankton, HPP = heterotrophic picoplankton, GSB = green sulfur bacteria, PSB = purple sulfur bacteria. The red circles and single rectangle correspond to the samples taken for each specific depth.

presented butanol dehydrogenase and the rest of butanol biosynthetic genes. Noteworthy were the Omnitrophota and Marinisomatota representatives, both presenting several specific species stratifications, which co-occurred at very variable abundances from 13.5 to 18 m. It must be noted that Nanoarchaeota (Woesearchaeales) and Patescibacteria (Gracillibacteria and Pacearchaeales) were particularly relevant from the deep chlorophyll maximum to the saline hypolimnion (12.5 to 13.5 m), coinciding with the highest abundance of anoxygenic phototrophs, and their metabolic repertoire for their very small genomes consisted basically of fermentative pathways (mainly lactate and formate biosynthesis). Finally, other prokaryotes such as *Izemoplasma* (previously classified as Tenericutes), Synergistales (Synergistota), Babeliales (Dependentiae), or Bipolaricaulota displayed variable relative abundances, though they just appeared from 14 m to the lake bottom, and would be mostly associated with S reducers.

In order to move between strata, some microbes such as PSB or various Desulfobacterota presented the capacity to develop gas vesicles and flagella. Some others did present only flagella, like anoxygenic Alphaproteobacterial phototrophs, methanotrophs or Spirochaetota. Noteworthy was the high abundance of CRISPR-Cas systems in the most abundant taxa of the lake, in particular in Desulfobacterota, PSB and GSB, Cloacimonadales, and *Methylovulum*. Overall, we showed a very specific microbial adaptation to the variable niches analyzed here that presented variable oxygen, redox states, and salinity concentrations.

Discussion

Meromictic lakes are without doubt a source of primary work in aquatic microbial ecology, albeit they have been mostly used as models to study certain microbes such as anoxygenic phototrophs and sulfate reducers, which are key players of these systems. Conversely, much less is known of their associated partners and how they interact and benefit from each other. In Lake El Tobar, the highest primary productivity of the lake concentrates around the deep chlorophyll maximum (Figs. 1, 2), where the interplay of light-salinity gradients allows for the potential interaction of many different microorganisms and metabolic processes that rarely occur in any other type of aquatic system. This productively active layer allows for the accumulation, by settling, of large amounts of organic matter in the deeper, aphotic, denser saltier layers, as observed from the increase of CDOM, easily utilizable substrates fueling specific metabolisms (see below). Another important factor of the lake is the increasing salinity with depth, which has been measured both by conductivity and by the pIs from predicted assembled proteomes. There is a general trend with the presence of more acidic predicted proteomes for salt-adapted bacteria/archaea and more neutral/basic proteomes for freshwaters, a pattern confirmed in the different gradients sampled in the lake along previously published metagenomes (Cabello-Yeves and Rodriguez-Valera 2019).

Regarding mechanisms of photoautotrophy, apart from the well-known epilimnetic phototrophs, the 12.5–13.5 m samples presented a huge concentration of *Rhodobacter* and *Rhodospirillum*-like species (see Figs. 4, 5), both of which have been previously noted in saline ecosystems as anoxygenic phototrophs (Madigan 2003; Koblížek 2015). Typically, *C. okenii* (Luedin et al. 2019) and other Purple sulfur bacteria (PSB) such as *Thiocystis*, *Lamprocystis*, *Thiocapsa/Thiohalocapsa* dominate meromictic systems (Zadereev et al. 2017) albeit here we found novel genus inside Chromatiaceae family (Supplementary Table S2). This novelty was also applied to Green sulfur bacteria (GSB), from which we detected a major bloom of novel *Chlorobium* spp. (Supplementary Table S2; Figs. 2, 4, 5). These microbes showed not only capabilities to fix C through anoxygenic photosynthesis, but also harbored several other metabolic pathways that made them very versatile to occupy different positions within the water column (Fig. 4). In particular, all PSB discovered here presented the capacity to move across the huge sulfide/light/DOC gradients either by gas vesicles, flagella, or both (Camacho and Vicente 1998; Rodrigo et al. 1999; Camacho et al. 2000), which allow them to optimize their position and photosynthetic behavior (Camacho and Vicente 1998). In addition, all PSB were able to perform S oxidation via the *sox* system and N fixation and elemental sulfur assimilation capacities were displayed by the most abundant *Chlorobium* and both PSB (*Chlorobium* sp. Tobar12.5 m-G31, Chromatiaceae Tobar14m-G20 and *Thiohalocapsa* sp. Tobar13m-G38). This is particularly relevant given that in Lake el Tobar there is no limitation in sulfate (Supplementary Table S1) and hydrogen sulfide (Vicente et al. 1993) where anoxygenic photosynthetic bacteria (GSB and PSB) mostly accumulate. On the other hand, we detected putative dissimilatory sulfate reduction genes (DSR) in GSB and PSB, which have been suggested as part of the elemental sulfur assimilation or as a reverse route to oxidize hydrogen sulfide to sulfite (Frigaard and Bryant 2008; Holkenbrink et al. 2011; Garcia et al. 2021).The presence of typically observed Desulfobacterota DSR genes in GSB and PSB opens up new perspectives for the study of (reverse) dissimilatory sulfite reductases in these bacteria. However, further phylogenetic and experimental evaluation is needed of whether the typical dissimilatory sulfate reduction conducted by Desulfobacterota/Firmicutes could be done by GSB and PSB. This is particularly important in conditions where anoxygenic photosynthesis (because of the absence of oxygen) and other chemolithotrophic metabolisms (lack of electron donors) would not be possible. Among the accompanying microbes of anoxygenic phototrophs, relatively high concentrations of Nanoarchaeota (Woesearchaeales; Castelle et al. 2018) and Patescibacteria (Gracillibacteria and Paceibacteria; Castelle et al. 2018; Parks et al. 2018) can be highlighted (Figs. 2, 4, 5), which lack key metabolic pathways for bacterial survival and

hence could perform an obligate fermentative lifestyle or even being attached to hosts as epibionts/symbionts to gather resources, as previously suggested (Hamm et al. 2019; McLean et al. 2020).

Potential metabolic networks are established among a huge variety of microbes. For instance, Desulfobacterota is a good example of a phylum that could be able to accept extracellular electrons in place of other chemical/organic electron donors, as noted previously in marine sediments (Skennerton et al. 2017). Most precisely, sulfate reducing bacteria outcompete methanogens for substrate uptake when sulfate is abundant to be used as electron acceptor (Lovley and Klug 1983; Oren 2011), as it occurs in Lake El Tobar deep layers. If we extrapolate these data, it appears that the high abundance of sulfate-reducers in Lake El Tobar has displaced the methanogens, which are extremely rare (no MAGs retrieved and < 0.1% of rRNA reads detected) in the water column though they can be found in the lake sediments (data not shown) though just accounting for 0.8% of the reads. Hence the competition between methanogens and sulfate-reducers for acetate in the monimolimnion is clearly dominated by the latter, which also can take a fundamental role in the potential metabolic network of the lake by consuming the H_2 produced by their associated partners, i.e., fermenters. Among all of these fermenters, it is noteworthy the presence of two novel species from Cloacimonadota phyla (previously known as WWE1), which have showed up in meromictic lakes as important carbon and sulfur recyclers (Hamilton et al. 2016) and appear to degrade propionic acid in syntrophic networks in bioreactors (Solli et al. 2014). In fact, the presence of novel microbes from lineages such as Acetothermia/Bipolaricaulota (Youssef et al. 2019; OP1), Marinisomatota (SAR406; Bertagnolli et al. 2017), Omnitrophicaeota (OP3), that were obtained as MAGs from the hypolimnetic and monimolimnetic waters of Lake El Tobar (Fig. 5), were previously found as well in a similar system in Romania (Ursu lake) as consortia in the euxinic waters of the lake (Baricz et al. 2020). Our data suggests that the abovementioned microbes, together with some other new species from Spirochaetota (Graber and Breznak 2004; Dong et al. 2018), Firmicutes, Dependentiae, Synergistota (Riviere et al. 2009), and Bacteroidota phyla (Fig. 5), are the key integrals of this peculiar type of systems. These taxa have been directly associated with syntrophic microbial networks (McInerney et al. 1981; Schnürer et al. 1996; Harmsen et al. 1998) with syntrophs (Summers et al. 2010; Dyksma and Gallert 2019), sulfate-reducers and/or methanogens (Hattori 2008; Stams and Plugge 2009; Skennerton et al. 2017). In particular, these microbes would recycle S and particulate and dissolved organic matter of the monimolimnion to form a very complex syntrophic network where mainly mixed-acid fermentations yielding lactate, ethanol, formate, succinate, hydrogen, and CO_2 as final products that are ultimately used by sulfate reducers (Firmicutes and Desulfobacterota). It must be noted that a somewhat similar microbial network was also reported for the euxinic waters of the Black Sea water column (Suominen et al. 2020; Cabello-Yeves et al. 2021).

One of the most remarkable metabolisms observed in the saline monimolimnion of Lake El Tobar was the H_2 production via hydrogenases or as product of mixed-acid fermentations (Supporting Information Fig. S1 and Figs. 3–5). Previous studies have shown the enhanced hydrogen production as a renewable biofuel in anaerobic reactors (Riviere et al. 2009) and several microbes have shown capabilities for dark fermentation and photoproduction of hydrogen (Nandi and Sengupta 1998). For instance, *Rhodobacter sphaeroides* has been used to increase H_2 biosynthesis (Tao et al. 2007) and several other microbes such as *Rhodospirillum rubrum*, *Clostridia*, *Cellulomonas*, or even *E. coli* have shown good production ratios (Nandi and Sengupta 1998). Lake El Tobar monimolimnion hosts a large number of microbes harboring hydrogenases and fermentative pathways leading to hydrogen production, conferring biotechnological importance in the context of renewable energy production. In this sense, another next generation biofuel is butanol. This compound is known to be produced by well-known Firmicutes such as class Clostridia (Jang et al. 2012). In this case, butanol production was still detectable (albeit much more restricted to specific taxa compared to hydrogen production) in microbes such as Firmicutes (Desulfatomaculales and *Izemoplasma*), a Spirochaetota and a Desulfobacterota (Syntrophia spp.) retrieved from Lake El Tobar anoxic waters.

The degree of resolution provided in our study, exemplified with ecological (meta)genomics and physical and chemical data, could serve as model case to study microbial ecology of meromictic lakes from various perspectives, as shown in Figs. 5, 6. This work represents a starting point to deepen into microbial associations such as chemotaxis and potential metabolic coupling in different layers from a single model habitat. This study has provided key ecological data that could give foundations to deepen into, for example, (1) the biotechnological production (bioreactors) of hydrogen and buthanol as biofuels used in the context of renewable energies; (2) relatively unknown microbial groups from which isolates could be obtained, that is, Spirochaeota, Cloacimonadota, Omnitrophota, and Marinisomatota; (iii) the chemotaxis and associations between these consortia with mesocosms and "in situ" experiments combined with other "omics" approaches (transcriptomics) complemented with long-reads.

Data availability statement

All data derived from this work is publicly available in the NCBI-Genbank databases.

References

Anantharaman, K., and others. 2016. Thousands of microbial genomes shed light on interconnected biogeochemical processes in an aquifer system. Nat. Commun. **7**: 13219.

Andrei, A.-Ş., and others. 2015. Contrasting taxonomic stratification of microbial communities in two hypersaline meromictic lakes. ISME J. **9**: 2642–2656.

APHA. 2005. Standard methods for the examination of water and wastewater. American Public Health Association/ American Water Works Association/Water Environment Federation.

Baricz, A., and others. 2020. Spatio-temporal insights into microbiology of the freshwater-to-hypersaline, oxic-hypoxic-euxinic waters of Ursu Lake. Environ. Microbiol. **23**: 3523–3540.

Barreiro-Lostres, F., E. Brown, A. Moreno, M. Morellón, M. Abbott, A. Hillman, S. Giralt, and B. Valero-Garcés. 2015. Sediment delivery and lake dynamics in a Mediterranean mountain watershed: Human-climate interactions during the last millennium (El Tobar Lake record, Iberian range, Spain). Sci. Total Environ. **533**: 506–519.

Benoit, G. 2015. Simka: Fast kmer-based method for estimating the similarity between numerous metagenomic datasets. RCAM.

Bertagnolli, A. D., C. C. Padilla, J. B. Glass, B. Thamdrup, and F. J. Stewart. 2017. Metabolic potential and in situ activity of marine Marinimicrobia bacteria in an anoxic water column. Environ. Microbiol. **19**: 4392–4416.

Biderre-Petit, C., N. Taib, H. Gardon, C. Hochart, and D. Debroas. 2019. New insights into the pelagic microorganisms involved in the methane cycle in the meromictic Lake Pavin through metagenomics. FEMS Microbiol. Ecol **95**: fiy183.

Boronat, M. D., and M. R. Miracle. 1997. Size distribution of Daphnia longispina in the vertical profile. Hydrobiologia **360**: 187–196.

Buchfink, B., C. Xie, and D. H. Huson. 2015. Fast and sensitive protein alignment using DIAMOND. Nat. Methods **12**: 59–60.

Buck, M., and others. 2021. Comprehensive dataset of shotgun metagenomes from oxygen stratified freshwater lakes and ponds. Sci Data **8**: 1–10.

Cabello-Yeves, P. J., R. Ghai, M. Mehrshad, A. Picazo, A. Camacho, and F. Rodriguez-Valera. 2017. Reconstruction of diverse Verrucomicrobial genomes from metagenome datasets of freshwater reservoirs. Front. Microbiol. **8**: 2131. doi:10.3389/fmicb.2017.02131

Cabello-Yeves, P. J., T. I. Zemskaya, R. Rosselli, F. H. Coutinho, A. S. Zakharenko, V. V. Blinov, and F. Rodriguez-Valera. 2018. Genomes of novel microbial lineages assembled from the sub-ice waters of Lake Baikal. Appl. Environ. Microbiol. **84**: e02132-17.

Cabello-Yeves, P. J., and F. Rodriguez-Valera. 2019. Marine-freshwater prokaryotic transitions require extensive changes in the predicted proteome. Microbiome **7**: 117. doi:10.1186/s40168-019-0731-5

Cabello-Yeves, P. J., T. I. Zemskaya, A. S. Zakharenko, M. V. Sakirko, V. G. Ivanov, R. Ghai, and F. Rodriguez-Valera. 2019. Microbiome of the deep Lake Baikal, a unique oxic bathypelagic habitat. Limnol. Oceanogr. **65**: 1471–1488.

Cabello-Yeves, P. J., and others. 2021. The microbiome of the Black Sea water column analyzed by shotgun and genome centric metagenomics. Environ. microbiome **16**: 1–15.

Camacho, A., and E. Vicente. 1998. Carbon photoassimilation by sharply stratified phototrophic communities at the chemocline of Lake Arcas (Spain). FEMS Microbiol. Ecol. **25**: 11–22.

Camacho, A., E. Vicente, and M. R. Miracle. 2000. Spatio-temporal distribution and growth dynamics of phototrophic sulfur bacteria populations in the sulfide-rich Lake Arcas. Aquat. Sci. **62**: 334–349.

Camacho, A., J. Erez, A. Chicote, M. Florín, M. M. Squires, C. Lehmann, and R. Backofen. 2001. Microbial microstratification, inorganic carbon photoassimilation and dark carbon fixation at the chemocline of the meromictic Lake Cadagno (Switzerland) and its relevance to the food web. Aquat. Sci. **63**: 91–106.

Camacho, A., E. Vicente, L. J. Garcia-Gil, M. R. Miracle, M. D. Sendra, X. Vila, and C. M. Borrego. 2002. Factors determining changes in the abundance and distribution of micro-, nano-and picoplanktonic phototrophs in Lake El Tobar (Central Spain). Int. Vereinigung Theor. Angew. Limnol. Verhandlungen **28**: 613–619.

Camacho, A., A. Picazo, M. R. Miracle, and E. Vicente. 2003. Spatial distribution and temporal dynamics of picocyanobacteria in a meromictic karstic lake. Arch. Hydrobiol. Suppl. Algol. Stud. **109**: 171–184.

Camacho, A., X. A. Walter, A. Picazo, and J. Zopfi. 2017. Photoferrotrophy: Remains of an ancient photosynthesis in modern environments. Front. Microbiol. **8**: 323.

Castelle, C. J., C. T. Brown, K. Anantharaman, A. J. Probst, R. H. Huang, and J. F. Banfield. 2018. Biosynthetic capacity, metabolic variety and unusual biology in the CPR and DPANN radiations. Nat. Rev. Microbiol. **16**: 629–645.

Danza, F., N. Storelli, S. Roman, S. Lüdin, and M. Tonolla. 2017. Dynamic cellular complexity of anoxygenic phototrophic sulfur bacteria in the chemocline of meromictic Lake Cadagno. PloS One **12**: e0189510.

Danza, F., D. Ravasi, N. Storelli, S. Roman, S. Lüdin, M. Bueche, and M. Tonolla. 2018. Bacterial diversity in the water column of meromictic Lake Cadagno and evidence for seasonal dynamics. PloS One **13**: e0209743.

Di Nezio, F., C. Beney, S. Roman, F. Danza, A. Buetti-Dinh, M. Tonolla, and N. Storelli. 2021. Anoxygenic photo-and chemo-synthesis of phototrophic sulfur bacteria from an alpine meromictic lake. FEMS Microbiol. Ecol **97**: fiab010.

Dong, X., and others. 2018. Fermentative Spirochaetes mediate necromass recycling in anoxic hydrocarbon-contaminated habitats. ISME J. **12**: 2039–2050.

Dyksma, S., and C. Gallert. 2019. Candidatus Syntrophosphaera thermopropionivorans: A novel player

in syntrophic propionate oxidation during anaerobic digestion. Environ. Microbiol. Rep. **11**: 558–570.

Edgar, R. C. 2010. Search and clustering orders of magnitude faster than BLAST. Bioinformatics **26**: 2460–2461.

Eisen, J. A., and others. 2002. The complete genome sequence of *Chlorobium tepidum* TLS, a photosynthetic, anaerobic, green-sulfur bacterium. Proc. Natl. Acad. Sci. **99**: 9509–9514.

Frigaard, N.-U., and D. A. Bryant. 2008. Genomic insights into the sulfur metabolism of phototrophic green sulfur bacteria, p. 337–355. *In* R. Hell, C. Dahl, D. Knaff, T. Leustek [eds.], Sulfur metabolism in phototrophic organisms. Springer.

Garcia, S. L., and others. 2021. Freshwater Chlorobia exhibit metabolic specialization among cosmopolitan and endemic populations. Msystems **6**: e01196-20.

Garcia-Gil, L. J., E. Vicente, A. Camacho, C. M. Borrego, X. Vila, X. P. Cristina, and J. Rodriguez-Gonzalez. 1999. Vertical distribution of photosynthetic Sulphur bacteria linked to saline gradients in Lake\'El Tobar\'(Cuenca, Spain). Aquat. Microb. Ecol. **20**: 299–303.

Ghai, R., C. M. Mizuno, A. Picazo, A. Camacho, and F. Rodriguez-Valera. 2014. Key roles for freshwater Actinobacteria revealed by deep metagenomic sequencing. Mol. Ecol. **23**: 6073–6090.

Golterman, H. L. 2004. Methodological aspects, p. 183–207. *In* The chemistry of phosphate and nitrogen compounds in sediments. Springer. doi:10.1007/1-4020-2516-5

Graber, J. R., and J. A. Breznak. 2004. Physiology and nutrition of Treponema primitia, an H2/CO2-acetogenic spirochete from termite hindguts. Appl. Environ. Microbiol. **70**: 1307–1314.

Gulati, R. D., E. S. Zadereev, and A. G. Degermendzhi. 2017. Ecology of meromictic lakes. Springer.

Haft, D. H., B. J. Loftus, D. L. Richardson, F. Yang, J. A. Eisen, I. T. Paulsen, and O. White. 2001. TIGRFAMs: A protein family resource for the functional identification of proteins. Nucleic Acids Res. **29**: 41–43.

Hamilton, T. L., and others. 2014. Coupled reductive and oxidative sulfur cycling in the phototrophic plate of a meromictic lake. Geobiology **12**: 451–468.

Hamilton, T. L., R. J. Bovee, S. R. Sattin, W. Mohr, W. P. Gilhooly III, T. W. Lyons, A. Pearson, and J. L. Macalady. 2016. Carbon and sulfur cycling below the chemocline in a meromictic lake and the identification of a novel taxonomic lineage in the FCB superphylum, Candidatus Aegiribacteria. Front. Microbiol. **7**: 598.

Hamm, J. N., and others. 2019. Unexpected host dependency of Antarctic Nanohaloarchaeota. Proc. Natl. Acad. Sci. **116**: 14661–14670.

Harmsen, H. J. M., B. L. M. Van Kuijk, C. M. Plugge, A. D. L. Akkermans, W. M. De Vos, and A. J. M. Stams. 1998. Syntrophobacter fumaroxidans sp. nov., a syntrophic propionate-degrading sulfate-reducing bacterium. Int. J. Syst. Evol. Microbiol. **48**: 1383–1387.

Hattori, S. 2008. Syntrophic acetate-oxidizing microbes in methanogenic environments. Microbes Environ. **23**: 118–127.

Holkenbrink, C., S. O. Barbas, A. Mellerup, H. Otaki, and N.-U. Frigaard. 2011. Sulfur globule oxidation in green sulfur bacteria is dependent on the dissimilatory sulfite reductase system. Microbiology **157**: 1229–1239.

Hyatt, D., G.-L. Chen, P. F. LoCascio, M. L. Land, F. W. Larimer, and L. J. Hauser. 2010. Prodigal: Prokaryotic gene recognition and translation initiation site identification. BMC Bioinformatics **11**: 1.

Jang, Y.-S., A. Malaviya, C. Cho, J. Lee, and S. Y. Lee. 2012. Butanol production from renewable biomass by clostridia. Bioresour. Technol. **123**: 653–663.

Kadnikov, V. V., A. S. Savvichev, A. V. Mardanov, A. V. Beletsky, N. V. Ravin, and N. V. Pimenov. 2019. Metagenomic data of the microbial community of the chemocline layer of the meromictic subarctic Lake bolshie Hruslomeny, North European Russia. Data Brief **23**: 103800.

Kanehisa, M., and S. Goto. 2000. KEGG: Kyoto encyclopedia of genes and genomes. Nucleic Acids Res. **28**: 27–30.

Kanehisa, M., Y. Sato, and K. Morishima. 2016. BlastKOALA and GhostKOALA: KEGG tools for functional characterization of genome and metagenome sequences. J. Mol. Biol. **428**: 726–731.

Kang, D., F. Li, E. S. Kirton, A. Thomas, R. S. Egan, H. An, and Z. Wang. 2019. MetaBAT 2: An adaptive binning algorithm for robust and efficient genome reconstruction from metagenome assemblies. PeerJ Prepr **7**: e7359.

King, C. E., M. R. Miracle, and E. Vicente. 1995. Large hardy-Weinberg equilibrium deviations in the Daphnia longispina of lake El Tobar, p. 15–23. *In* P. Larsson, and L. J. Weider, [eds.], Cladocera as Model Organisms in Biology. Springer.

Koblížek, M. 2015. Ecology of aerobic anoxygenic phototrophs in aquatic environments. FEMS Microbiol. Rev. **39**: 854–870.

Kubo, K., H. Kojima, and M. Fukui. 2014. Vertical distribution of major sulfate-reducing bacteria in a shallow eutrophic meromictic lake. Syst. Appl. Microbiol. **37**: 510–519.

Langmead, B., and S. L. Salzberg. 2012. Fast gapped-read alignment with bowtie 2. Nat. Methods **9**: 357–359.

Langwig, M. V., V. De Anda, N. Dombrowski, K. W. Seitz, I. M. Rambo, C. Greening, A. P. Teske, and B. J. Baker. 2021. Large-scale protein level comparison of Deltaproteobacteria reveals cohesive metabolic groups. ISME J. **16**: 1–14.

Lauro, F. M., and others. 2011. An integrative study of a meromictic lake ecosystem in Antarctica. ISME J. **5**: 879–895.

Lê, S., J. Josse, and F. Husson. 2008. FactoMineR: An R package for multivariate analysis. J. Stat. Softw. **25**: 1–18.

Legendre, P., and M. J. Anderson. 1999. Distance-based redundancy analysis: Testing multispecies responses in

multifactorial ecological experiments. Ecological monographs **69**: 1–24.

Linz, A. M., S. He, S. L. R. Stevens, K. Anantharaman, R. R. Rohwer, R. R. Malmstrom, S. Bertilsson, and K. D. McMahon. 2018. Freshwater carbon and nutrient cycles revealed through reconstructed population genomes. PeerJ **6**: e6075.

Lovley, D. R., and M. J. Klug. 1983. Sulfate reducers can outcompete methanogens at freshwater sulfate concentrations. Appl. Environ. Microbiol. **45**: 187–192.

Lowe, T. M., and S. R. Eddy. 1997. tRNAscan-SE: A program for improved detection of transfer RNA genes in genomic sequence. Nucleic Acids Res. **25**: 955–964.

Luedin, S. M., and others. 2019. Draft genome sequence of Chromatium okenii isolated from the stratified alpine Lake Cadagno. Sci. Rep. **9**: 1–14.

Madigan, M. T. 2003. Anoxygenic phototrophic bacteria from extreme environments. Photosynth. Res. **76**: 157–171.

Marchler-Bauer, A., and others. 2016. CDD/SPARCLE: Functional classification of proteins via subfamily domain architectures. Nucleic Acids Res. **45**: D200–D203.

Marie, D., F. Partensky, S. Jacquet, and D. Vaulot. 1997. Enumeration and cell cycle analysis of natural populations of marine picoplankton by flow cytometry using the nucleic acid stain SYBR green I. Appl. Environ. Microbiol. **63**: 186–193.

Martín-Cuadrado, A.-B., P. López-García, J.-C. Alba, D. Moreira, L. Monticelli, A. Strittmatter, G. Gottschalk, and F. Rodríguez-Valera. 2007. Metagenomics of the deep Mediterranean, a warm bathypelagic habitat. PloS One **2**: e914.

McInerney, M. J., M. P. Bryant, R. B. Hespell, and J. W. Costerton. 1981. Syntrophomonas wolfei gen. Nov. sp. nov., an anaerobic, syntrophic, fatty acid-oxidizing bacterium. Appl. Environ. Microbiol. **41**: 1029–1039.

McLean, J. S., and others. 2020. Acquisition and adaptation of ultra-small parasitic reduced genome bacteria to mammalian hosts. Cell Rep. **32**: 107939.

Mehrshad, M., M. M. Salcher, Y. Okazaki, S. Nakano, K. Šimek, A.-S. Andrei, and R. Ghai. 2018. Hidden in plain sight—Highly abundant and diverse planktonic freshwater Chloroflexi. Microbiome **6**: 176.

Miracle, M. R., E. Vicente, and C. Pedrós-Alió. 1992. Biological studies of Spanish meromictic and stratified karstic lakes. Limnetica **8**: 59–77.

Miracle, M. R., J. Armengol-Díaz, and M. J. Dasí. 1993. Extreme meromixis determines strong differential planktonic vertical distributions. Int. Vereinigung Theor. Angew. Limnol. Verhandlungen **25**: 705–710.

Nandi, R., and S. Sengupta. 1998. Microbial production of hydrogen: An overview. Crit. Rev. Microbiol. **24**: 61–84.

Nawrocki, E. P., and S. R. Eddy. 2010. SSU-align: A tool for structural alignment of SSU rRNA sequences. https://selab.janelia.org/software

Okazaki, Y., Y. Nishimura, T. Yoshida, H. Ogata, and S. Nakano. 2019. Genome-resolved viral and cellular metagenomes revealed potential key virus-host interactions in a deep freshwater lake. Environ. Microbiol. **21**: 4740–4754.

Oren, A. 2011. Thermodynamic limits to microbial life at high salt concentrations. Environ. Microbiol. **13**: 1908–1923.

Overbeek, R., and others. 2013. The SEED and the rapid annotation of microbial genomes using subsystems technology (RAST). Nucleic Acids Res. **42**: D206–D214.

Panwar, P., and others. 2020. Influence of the polar light cycle on seasonal dynamics of an Antarctic lake microbial community. Microbiome **8**: 1–24.

Parks, D. H., M. Imelfort, C. T. Skennerton, P. Hugenholtz, and G. W. Tyson. 2015. CheckM: Assessing the quality of microbial genomes recovered from isolates, single cells, and metagenomes. Genome Res. **25**: 1043–1055.

Parks, D. H., M. Chuvochina, D. W. Waite, C. Rinke, A. Skarshewski, P.-A. Chaumeil, and P. Hugenholtz. 2018. A standardized bacterial taxonomy based on genome phylogeny substantially revises the tree of life. Nat. Biotechnol. **36**: 996–1004.

Peduzzi, S., M. Tonolla, and D. Hahn. 2003. Vertical distribution of sulfate-reducing bacteria in the chemocline of Lake Cadagno, Switzerland, over an annual cycle. Aquat. Microb. Ecol. **30**: 295–302.

Peng, Y., H. C. M. Leung, S.-M. Yiu, and F. Y. L. Chin. 2012. IDBA-UD: A de novo assembler for single-cell and metagenomic sequencing data with highly uneven depth. Bioinformatics **28**: 1420–1428.

Philippi, M., and others. 2021. Purple sulfur bacteria fix N2 via molybdenum-nitrogenase in a low molybdenum Proterozoic Ocean analogue. Nat. Commun. **12**: 4774.

Picazo, A., C. Rochera, E. Vicente, M. R. Miracle, and A. Camacho. 2013. Spectrophotometric methods for the determination of photosynthetic pigments in stratified lakes: A critical analysis based on comparisons with HPLC determinations in a model lake. Limnetica **32**: 139–158.

Quast, C., E. Pruesse, P. Yilmaz, J. Gerken, T. Schweer, P. Yarza, J. Peplies, and F. O. Glöckner. 2012. The SILVA ribosomal RNA gene database project: Improved data processing and web-based tools. Nucleic Acids Res. **41**: D590–D596.

Rice, P., I. Longden, and A. Bleasby. 2000. EMBOSS: The European molecular biology open software suite. Trends Genet. **16**: 276–277.

Riviere, D., and others. 2009. Towards the definition of a core of microorganisms involved in anaerobic digestion of sludge. ISME J. **3**: 700–714.

Rodrigo, M. A., A. Camacho, E. Vicente, and M. R. Miracle. 1999. Microstratified vertical distribution and migration of phototrophic microorganisms during a diel cycle in Lake Arcas-2 (Spain). Arch. für Hydrobiol. **145**: 497–512.

Saini, J. S., and others. 2022. Bacterial, phytoplankton, and viral distributions and their biogeochemical contexts in

meromictic Lake Cadagno offer insights into the Proterozoic Ocean microbial loop. MBio **13**: e00052-22.

Schnürer, A., B. Schink, and B. H. Svensson. 1996. Clostridium ultunense sp. nov., a mesophilic bacterium oxidizing acetate in syntrophic association with a hydrogenotrophic methanogenic bacterium. Int. J. Syst. Evol. Microbiol. **46**: 1145–1152.

Skennerton, C. T., K. Chourey, R. Iyer, R. L. Hettich, G. W. Tyson, and V. J. Orphan. 2017. Methane-fueled syntrophy through extracellular electron transfer: Uncovering the genomic traits conserved within diverse bacterial partners of anaerobic methanotrophic archaea. MBio **8**: e00530-17.

Solli, L., O. E. Håvelsrud, S. J. Horn, and A. G. Rike. 2014. A metagenomic study of the microbial communities in four parallel biogas reactors. Biotechnol. Biofuels **7**: 146.

Stams, A. J. M., and C. M. Plugge. 2009. Electron transfer in syntrophic communities of anaerobic bacteria and archaea. Nat. Rev. Microbiol. **7**: 568–577.

Storelli, N., S. Peduzzi, M. M. Saad, N.-U. Frigaard, X. Perret, and M. Tonolla. 2013. CO2 assimilation in the chemocline of Lake Cadagno is dominated by a few types of phototrophic purple sulfur bacteria. FEMS Microbiol. Ecol. **84**: 421–432.

Summers, Z. M., H. E. Fogarty, C. Leang, A. E. Franks, N. S. Malvankar, and D. R. Lovley. 2010. Direct exchange of electrons within aggregates of an evolved syntrophic coculture of anaerobic bacteria. Science **330**: 1413–1415.

Suominen, S., N. Dombrowski, J. S. Sinninghe Damsté, and L. Villanueva. 2020. A diverse uncultivated microbial community is responsible for organic matter degradation in the Black Sea sulphidic zone. Environ. Microbiol. **23**: 2709–2728.

Tao, Y., Y. Chen, Y. Wu, Y. He, and Z. Zhou. 2007. High hydrogen yield from a two-step process of dark-and photo-fermentation of sucrose. Int. J. Hydrogen Energy **32**: 200–206.

Tatusov, R. L., and others. 2001. The COG database: New developments in phylogenetic classification of proteins from complete genomes. Nucleic Acids Res. **29**: 22–28.

Tonolla, M., A. Demarta, S. Peduzzi, D. Hahn, and R. Peduzzi. 2000. In situ analysis of sulfate-reducing bacteria related to Desulfocapsa thiozymogenes in the chemocline of meromictic Lake Cadagno (Switzerland). Appl. Environ. Microbiol. **66**: 820–824.

Tonolla, M. et al. (2017). Lake Cadagno: Microbial life in crenogenic meromixis. *In* Gulati, R., Zadereev, E., Degermendzhi, A. [eds.], Ecology of meromictic Lakes. Ecological studies, vol 228. Springer. doi:10.1007/978-3-319-49143-1_7

Tran, P., A. Ramachandran, O. Khawasek, B. E. Beisner, M. Rautio, Y. Huot, and D. A. Walsh. 2018. Microbial life under ice: Metagenome diversity and in situ activity of Verrucomicrobia in seasonally ice-covered lakes. Environ. Microbiol. **20**: 2568–2584.

Tran, P. Q., and others. 2021. Depth-discrete metagenomics reveals the roles of microbes in biogeochemical cycling in the tropical freshwater Lake Tanganyika. ISME J. **15**: 1–16.

Vavourakis, C. D., A.-S. Andrei, M. Mehrshad, R. Ghai, D. Y. Sorokin, and G. Muyzer. 2018. A metagenomics roadmap to the uncultured genome diversity in hypersaline soda lake sediments. Microbiome **6**: 168.

Vavourakis, C. D., M. Mehrshad, C. Balkema, R. Van Hall, A.-Ş. Andrei, R. Ghai, D. Y. Sorokin, and G. Muyzer. 2019. Metagenomes and metatranscriptomes shed new light on the microbial-mediated sulfur cycle in a Siberian soda lake. BMC Biol. **17**: 69.

Vicente, E., A. Camacho, and M. A. Rodrigo. 1993. Morphometry and physico-chemistry of the crenogenic meromictic Lake El Tobar (Spain). Int. Vereinigung Theor. Angew. Limnol. Verhandlungen **25**: 698–704.

Walter, X. A., A. Picazo, M. R. Miracle, E. Vicente, A. Camacho, M. Aragno, and J. Zopfi. 2014. Phototrophic Fe (II)-oxidation in the chemocline of a ferruginous meromictic lake. Front. Microbiol. **5**: 713.

Wetzel, R. G. 2001. Limnology: Lake and river ecosystems. Gulf Professional Publishing.

Wu, Y.-T., and others. 2018. Comprehensive insights into composition, metabolic potentials, and interactions among archaeal, bacterial, and viral assemblages in meromictic Lake Shunet in Siberia. Front. Microbiol. **9**: 1763.

Yau, S., F. M. Lauro, T. J. Williams, M. Z. DeMaere, M. V. Brown, J. Rich, J. A. E. Gibson, and R. Cavicchioli. 2013. Metagenomic insights into strategies of carbon conservation and unusual sulfur biogeochemistry in a hypersaline Antarctic lake. ISME J. **7**: 1944–1961.

Youssef, N. H., and others. 2019. The wood–Ljungdahl pathway as a key component of metabolic versatility in candidate phylum Bipolaricaulota (Acetothermia, OP1). Environ. Microbiol. Rep. **11**: 538–547.

Zadereev, E. S., R. D. Gulati, and A. Camacho. 2017. Biological and ecological features, trophic structure and energy flow in meromictic lakes, p. 61–86. *In* R. Gulati, E. Zadereev, A. and Degermendzhi, [eds.], Ecology of meromictic lakes. Springer.

Acknowledgments

This work has been mainly funded by project PID2019-104742RB-I00, plus, partly co-funded, by projects TED2022-132199B-100 and PDC2022-133205-100, all of them granted by the Agencia Estatal de Investigacion (AEI) of Spain, to AC, the last two included in the "Recovery, Transformation, and Resilience Plan", funded by the European Union - New generation EU. It was also partly co-funded by grant "VIREVO" CGL2016-76273-P [MCI/AEI/FEDER, EU] (co-funded with FEDER funds) from the Spanish Ministerio de Ciencia e Innovación, as well as "HIDRAS3" PROMETEO/2019/009 from Generalitat Valenciana granted to both researchers. FRV was also a beneficiary of the 5top100-program of the Ministry for Science and Education of Russia. PJC-Y was supported by a APOSTD/2019/009 Post-Doctoral Fellowship from Generalitat Valenciana

and is currently supported by a Post-Doctoral Fellowship from the Fundación Alfonso Martín Escudero, Spain.

Conflict of Interest

The authors declare that they have no competing interest.

Submitted 01 December 2022
Revised 25 April 2023
Accepted 23 September 2023

Associate editor: Osvaldo Ulloa